Chem Soc Rev

This article was published as part of the

Hybrid materials themed issue

Guest editors Clément Sanchez, Kenneth J. Shea and Susumu Kitagawa

Please take a look at the issue 2 2011 table of contents to access other reviews in this themed issue

Chem Soc Rev

Dynamic Article Links

Cite this: *Chem. Soc. Rev.*, 2011, **40**, 536–549

www.rsc.org/csr

TUTORIAL REVIEW

Progress on lanthanide-based organic–inorganic hybrid phosphors†

Luís D. Carlos,*[a] Rute A. S. Ferreira,[a] Verónica de Zea Bermudez,[b] Beatriz Julián-López[c] and Purificación Escribano*[c]

Received 6th August 2010
DOI: 10.1039/c0cs00069h

Research on organic–inorganic hybrid materials containing trivalent lanthanide ions (Ln^{3+}) is a very active field that has rapidly shifted in the last couple of years to the development of eco-friendly, versatile and multifunctional systems, stimulated by the challenging requirements of technological applications spanning domains as diverse as optics, environment, energy, and biomedicine. This *tutorial review* offers a general overview of the myriad of advanced Ln^{3+}-based organic–inorganic hybrid materials recently synthesised, which may be viewed as a major innovation in areas of phosphors, lighting, integrated optics and optical telecommunications, solar cells, and biomedicine.

Introduction

Interest in Ln^{3+}-containing organic–inorganic hybrid materials—noticeably during the last decade—has occurred together with the co-occurrence of materials with multifunctional, versatile and modulated properties.[1] The tailoring of these hybrid structures (and hence of their corresponding properties) passes for the capability of exploiting the synergy between the intrinsic characteristics of sol–gel derived organic–inorganic hybrid hosts—such as highly controlled purity, versatile shaping and patterning, easy control of the refractive index, photosensitivity, encapsulation of large amounts of isolated emitting centres, mechanical, optical and/or electronic properties, thermal and chemical stability, biocompatibility, hydrophobic-hydrophilic balance—and the luminescence features of Ln^{3+} ions—such as high luminescence quantum yield, narrow bandwidth, long-lived emission, large Stokes shifts, and ligand-dependent luminescence sensitization.[2–4] All of these features offer excellent prospects for designing

[a] *Department of Physics, CICECO, University of Aveiro, Campus Universitário de Santiago, 3810–193 Aveiro, Portugal. E-mail: lcarlos@ua.pt; Fax: 351 234 378197; Tel: 351 234 370946*
[b] *Departamento de Química, CQ-VR, Universidade de Trás-os-Montes e Alto Douro, 5001-801 Vila Real, Portugal*
[c] *Departamento de Química Inorgánica y Orgánica, Universitat Jaume I, Avda. Sos Baynat s/n, 12071, Castellón, Spain. E-mail: escriban@qio.uji.es; Fax: +34 964 728214; Tel: +34 964 728247*
† Part of the themed issue on hybrid materials.

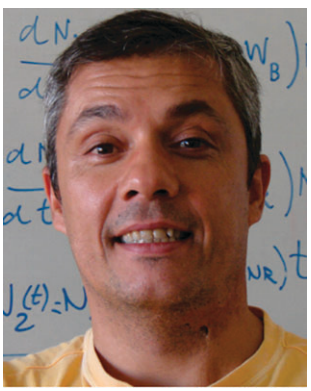

Luís D. Carlos

Luís Carlos, born in 1964, got his PhD in physics from the University of Évora in 1995 working on photoluminescence of polymer electrolytes incorporating lanthanide salts. In 1996 he joined the Department of Physics at the University of Aveiro, where he is now Full Professor. Since 2009 he has been the vice-director of the Centre for Research in Ceramics and Composite Materials (CICECO) at Aveiro, Portugal. His current scientific interests include: light emission of organic–inorganic hybrids, silicates, nanocrystals and metal organic frameworks; applications of organic–inorganic hybrids in solid-state lighting and integrated optics; and luminescent/magnetic nanoparticles as new probes for multimodal imaging.

Rute A. S. Ferreira

Rute A. S. Ferreira, born in 1974, obtained a first degree in Physical Engineering in 1997 and in 2002, a PhD in Physics at the University of Aveiro, Portugal. She has been an Auxiliary Researcher at the Centre for Research in Ceramics and Composite Materials (CICECO) at Aveiro since 2003. Her research interests are the photoluminescence features of functional lanthanide-doped organic–inorganic hybrids and the production and characterization of hybrid-based components for integrated optics and optical telecommunications.

new luminescent materials with enhanced desired characteristics and high added value for specific targeted applications, thus opening exciting new directions in materials science and related technologies, with noteworthy results in the ecofriendly integration, miniaturization and multifunctionalization of devices.

The present tutorial review aims at describing the latest progress of the photonic properties of Ln^{3+}-containing organic–inorganic hybrids. It can be considered as being a follow up of three reviews on the same theme published in 2008 and 2009.[2–4] In view of the current trends of the subject, and balancing the literature published over the last year, the topics discussed below focus on the application of Ln^{3+}-containing organic–inorganic hybrids as phosphors, in lighting, in integrated optics and optical telecommunications, in solar cells, and in biomedicine. Selected latest developments in these areas will be discussed, future prospects will be highlighted and main research targets will be presented.

Verónica de Zea Bermudez

Verónica de Zea Bermudez, born in 1962, obtained a first degree in chemical engineering and an MSc degree in chemistry of catalytic processes at the Instituto Superior Técnico, Portugal. She received a PhD degree in electrochemistry in 1992 from the Institut Polytechnique de Grenoble, France, under the supervision of Christiane Poinsignon. In 1993 she joined the University of Trás-os-Montes e Alto Douro, where she is now Professor of Materials Chemistry in the Department of Chemistry. Her current scientific interests include: amorphous and hierarchically structured ordered organic/inorganic hybrid materials; sol–gel chemistry and self-assembly routes; biomineralisation and biomaterials; and infrared and Raman spectroscopy.

Hybrids as phosphors

The incorporation of Ln^{3+} complexes into organic–inorganic hybrid hosts with the purpose of producing highly efficient blue-, green- and red-emitting phosphors is of widespread interest in materials science, due to their important roles in display devices and lighting technologies. Full-colour phosphors may in principle be obtained by controlling the relative amount of these monochromatic emissions. This topic is undoubtedly the one most addressed in the literature concerning applications of Ln^{3+}-based hybrid structures. The significant number of published examples that can be found were extensively reviewed elsewhere.[2–4] Here we will emphasise some illustrative examples in which the hybrid host belongs to one of the following classes: amine- and amide-functionalized matrices;[5,6] organosilicas;[7,8] mesostructured materials;[9,10] ionogels;[11,12] and ligand-decorated nanoparticles (NPs).[13–15]

Besides the intra-4*f* lines, the emission spectra of Ln^{3+}-based amine- and amide-functionalized organic–inorganic hybrids display a broad emission in the blue-green spectral region (380–550 nm) ascribed to the hybrid host. This large broad band, already observed in the nondoped matrices, results from a convolution of the emission originated in the cross-linkages between the organic and inorganic counter parts with electron-hole recombinations occurring in the siloxane nanoclusters.[4–6] The relative intensity between the hybrid host broad band and the intra-4*f* lines strongly depends on the activation/deactivation of the host-to-Ln^{3+} energy-transfer processes,[4] allowing, therefore, the fine-tuning of the hybrids emission chromaticity across the Commission Internationale d'Eclairage (CIE) diagram. This emission-colour fine tuning along the CIE chromaticity diagram can be also modulated by chemical factors (Ln^{3+} concentration, polymer chain length, nature of the cross-linkage and anion type) and physical parameters (excitation wavelength and temperature), Fig. 1.

A ligand-assisted rational design based on the synergy between the absorption ability of the ligand chromophores (essentially β-diketonate units) and the ligand-to-hybrid energy

Beatriz Julián-López

Beatriz Julián-López, born in 1977, obtained her BSc degree in chemistry in 1999 at the Jaume I University of Castellón, Spain, where she also received her PhD in Materials Chemistry (2003) under the supervision of E. Cordoncillo, P. Escribano and C. Sanchez. In 2004 she undertook postdoctoral research in the group of C. Sanchez at Pierre et Marie Curie University-CNRS, Paris. She has been "Ramon y Cajal" Researcher at Jaume I University since 2007. Her main interest is the design of novel multifunctional hybrid organic–inorganic materials, textured at different scales, by combining sol–gel, solvothermal and self-assembling processes, for optics and ceramics.

Purificación Escribano

Purificación Escribano has more than 20 years experience in applied materials research. She received her PhD in 1982 in Inorganic Chemistry, at the University of Valencia. She is Full Professor of Inorganic Chemistry and leads a research group at Jaume I University of Castellon, Spain. Her interests include the synthesis, characterization and application of ceramic pigments with low environmental impact by using lanthanide ions and soft chemistry routes to prepare tailored hybrid organic–inorganic nanomaterials with interesting optical properties.

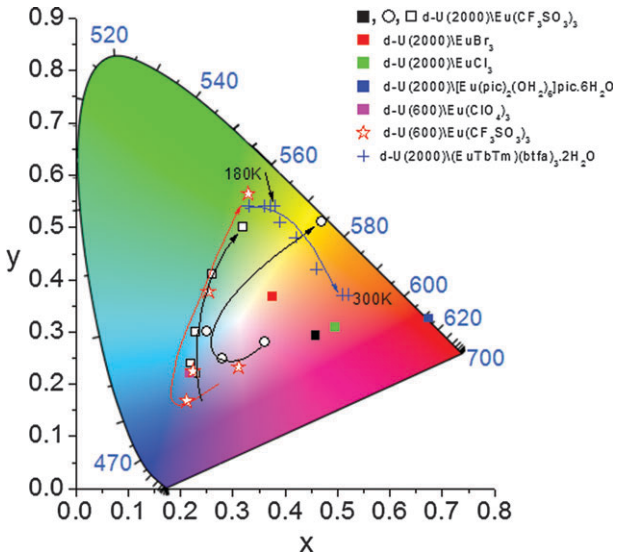

Fig. 1 CIE chromaticity diagram showing the (x,y) emission color coordinates of d-U(2000) and d-U(600) di-ureasils incorporating distinct Eu^{3+} compounds. The lines through the data are guides for the eye, indicating changes in the (x,y) coordinates as a function of Eu^{3+} concentration (red arrow) and excitation wavelength (black arrows). For d-U(600)\Eu(CF_3SO_3)$_3$, the Eu^{3+} concentration decreases from 4.8 to 0.6% (relatively to the hybrids total mass) and for d-U(2000)\Eu(CF_3SO_3)$_3$, the excitation wavelength increases from 360 to 460 nm (open squares, Eu^{3+} concentration of 1.2%) and from 280 to 501 nm (circles, Eu^{3+} concentration of 2.8%). For d-U(2000)\(Eu,Tb,Tm)(btfa)$_3$·2H_2O, complex molar proportion of Ln(btfa)$_3$·2H_2O, Ln = Eu, Tb, and Tm, of 0.05, 0.15 and 0.80, respectively, the temperature was varied between 14–300 K at 377 nm (blue line) (Adapted with permission from ref. 4, copyright 2009 Wiley InterScience.)

transfer, was proposed to optimize the Ln^{3+} sensitization process contributing, therefore, to the improvement of the emission quantum yield (*e.g.*, 0.60 ± 0.06 for a Eu^{3+}-containing di-ureasil, the hybrid material that displays the highest emission quantum yield reported so far).[16] The basic principle of this new synthetic approach is based on the suitable design of the precursor complex: the Ln^{3+}-first coordination shell should comprise, not only oxygen or/and nitrogen atoms included in high absorption, light-harvesting ligands for efficient emission sensitization, but also labile molecules (*e.g.* water, methanol and ethanol) that can, after incorporation, be easily replaced by the functional groups of the hybrid structure. An accurate choice of the ligands, permitting that the hybrid network itself acts as a ligand, is crucial for the success of that rational design. In fact, the steric hindrance between the polymer chains of the hybrid structure and bulky highly chelating ligands (*e.g.*, phen and bpy, where phen is 1,10-phenanthroline and bpy is 2,2′-bipyridine), normally promotes the expulsion of these ligands from the Ln^{3+} first coordination shell and their replacement by quenching water molecules, with the subsequent reduction of the emission quantum yield.[4,16]

Light-harvesting Eu^{3+}- and Tb^{3+}-based complexes anchored onto the surface of silica particles or layers have also been largely explored throughout the past decade. The grafting of the emitting guest molecules to the host hybrid framework is performed either through a one-step process or a post-synthesis step (taking advantage of the presence of residual –OH groups that can provide reaction sites for chemical grafting). An interesting example, addressed by Armelao *et al.*,[7] is that of Eu^{3+}- and Tb^{3+}-based complexes composed of a macrocyclic ligand, functionalized with distinct light-harvesting units (*e.g.* phen and acetophenone derivatives), anchored to silica layers. Independently of the Eu^{3+}/Tb^{3+} concentration and of the type of light-harvesting ligands employed, homogeneous, transparent, and crack-free well-adherent to the substrates as-deposited layers were produced. Moreover, significant luminescence brightness with quantum yields up to 0.25 for Eu^{3+}- and 0.45 for Tb^{3+}-based hybrids could be reached (Fig. 2).

Other examples of organic–inorganic hybrids containing organic components covalently bonded to a silica-based skeleton and possessing functional groups prone to participating in Ln^{3+} coordination were investigated by Yan *et al.* during the past decade.[8] A more recent approach involves the synthesis of functional molecular bridges that can coordinate to Ln^{3+} and simultaneously form inorganic Si–O–Si networks with silicon alkoxides (*e.g.* tetraethoxysilane, (TEOS), 3-methacryloxypropyltrimethoxysilane (MAPTMS), 3-aminopropyltriethoxysilane (APTS) and 3-glycidoxypropyltrimethoxysilane (GPTMS)) *via* hydrolysis and condensation processes. Selected *N*-heterocyclic ligands (*e.g.* phen and bpy) were used as light harvesting additional ligands.[8]

Full-colour phosphors based on mesophase silicates, processed as thin films and incorporating Eu^{3+}- and Tb^{3+}-based complexes and organic ligands were introduced by Bae *et al.*[9] The complexes act as green (Tb^{3+}) and red (Eu^{3+}) emitter components, whereas the organic ligands give rise to blue emission, acting simultaneously as photosensitizers. The colour can be tuned, therefore, by changing the relative amount of Eu^{3+}, Tb^{3+} and organic photosensitizers (thus affecting the energy transfer between the various components), resulting in a multicoloured photoluminescence, including white light at room temperature (Fig. 3). The thin films display quantum yield values between 0.04 and 0.35, and the mesophase matrix permits the local separation of organic and inorganic regions, prevents dopant aggregation and ensures the chemical inertness and porosity control of the silicate scaffold.[9]

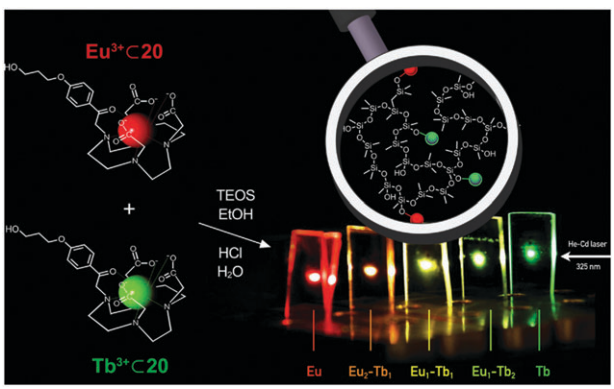

Fig. 2 Colours emitted by silica layers containing different ratios of Eu^{3+} and Tb^{3+} complexes. (Reproduced with permission from ref. 7, copyright 2010 Elsevier.)

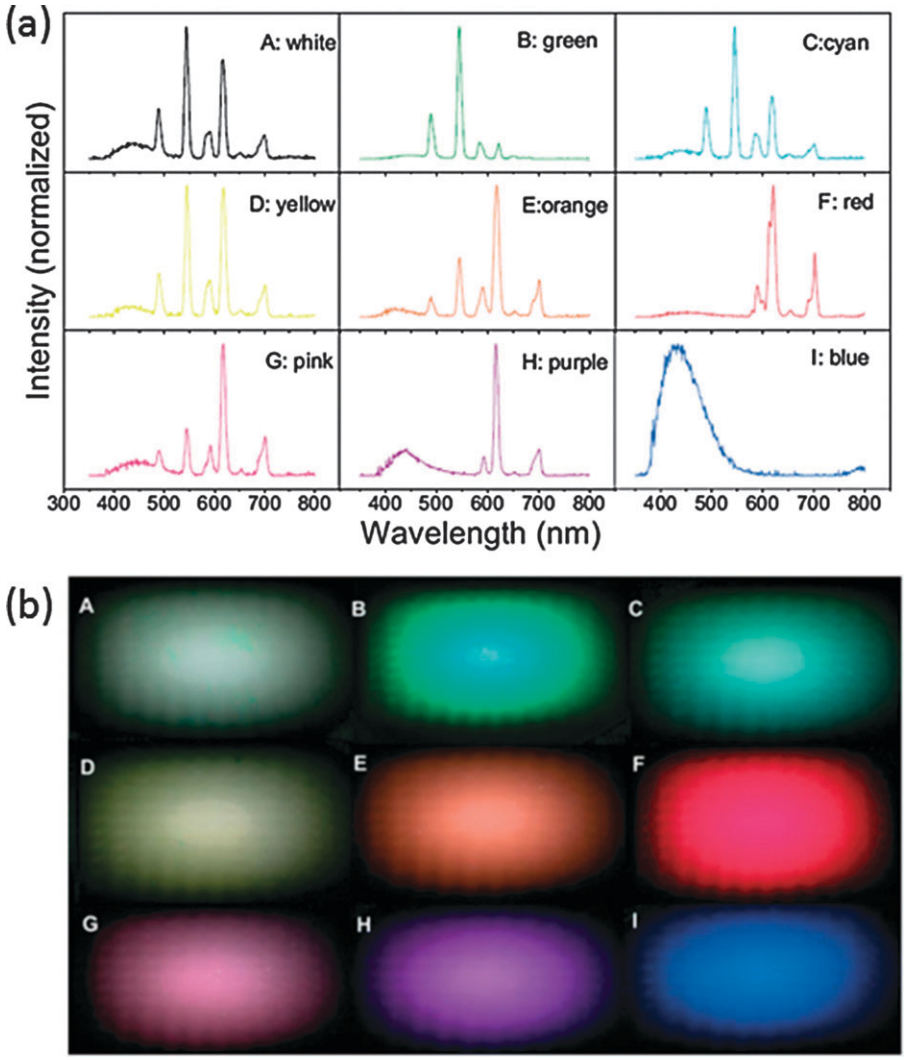

Fig. 3 (a) Photoluminescence spectra of the mesophase thin films incorporated with various ratios of luminescent dopants at room temperature with UV excitation at 290 nm and (b) photographs of the photoluminescence colors from the mesophase thin films with the UV excitation using a Hg/Xe lamp as the excitation source. (A–I) stand for the mole ratio of Eu/Tb/phen/salicylic acid of 0.5/1.5/4.5/7.5, 0/2/0/6, 0.75/1.25/2.25/3.75, 1/1/3/3, 1/0.5/3/1.5, 2/0/6/0, 2/0.5/6/1.5, 1/0/2.25/3.75 and 0/0/0/7.5), respectively. (Adapted with permission from ref. 9, copyright 2007 Wiley InterScience.)

With this elegant approach, full-colour phosphors can be proposed in order to overcome the difficulty of synthesizing efficient Ln^{3+}-based blue emitter complexes. However, the distinct nature of the three emitters gives rise to some drawbacks concerning the material's luminescence dynamics, *e.g.*, the photostability of the three colours under UV excitation is significantly different, inducing a degradation of the material colour coordinates during the irradiation time.

Mesoporous organic–inorganic hybrids displaying interesting phosphor characteristics were reported by Park *et al.*[10] and Wang *et al.*[17] Park *et al.* proposed UV sensors, based on Tm^{3+}-, Tb^{3+}- and Eu^{3+}-containing transparent and oriented periodic mesoporous monoliths (synthesized through surfactant-templated assembly) that emit blue, green or red emissions, respectively, upon UV irradiation (Fig. 4).[10] Wang *et al.* synthesised dense, homogeneous, well-oriented, stable, and highly organized open-channel monolayers of zeolite L microcrystals, using an organic–inorganic functional linker capable of coordinating and sensitizing Ln^{3+} ions and also of self-assembling through hydrogen bonding.[17] The emission colour of the resulting layers can be fine-tuned by changing: (1) the amount and type of the Ln^{3+} ions coordinated to the linker, (2) the guest species inside the channels of the zeolite host, and (3) the excitation wavelength, thus opening exciting expectations for sensing purposes.

Luminescent ionogels are a quite recent class of interesting organic–inorganic hybrid phosphors, consisting of an ionic liquid incorporating Ln^{3+} complexes, confined into silica-based matrices.[11,12] Ionogels are obtained as easy-shaped monoliths, featuring the transparency of silica, the good ionic conductivity performances of ionic liquids and the characteristic emission of the Ln^{3+} complexes, which, despite the confinement, remain essentially unchanged relative to that of their precursors. Examples include visible and near-infrared (NIR) emissions of mixtures of ionic liquids and Ln^{3+} tetrakis β-diketonates, confined inside the nano-sized pores of a silica

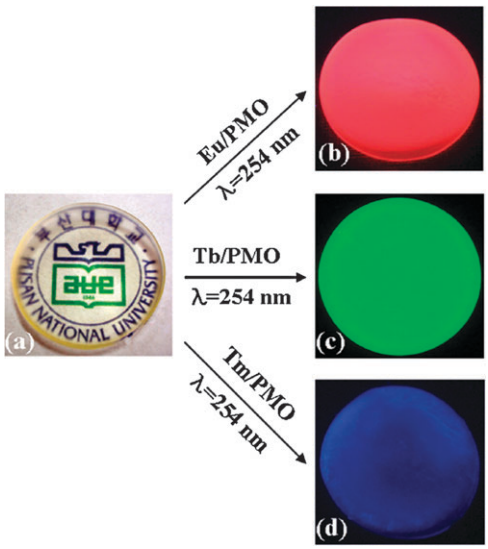

Fig. 4 Photographs of as-synthesized Eu^{3+}-, Tb^{3+}, and Tm^{3+}-doped PMO monoliths upon (a) day light illumination and (b), (c) and (d) 254 nm irradiation. (Reproduced with permission from ref. 10, copyright 2008 Elsevier.)

network,[11] and grafted to functionalized ordered MCM-41 mesoporous silica.[12]

Embedding Ln^{3+} ions in hybrid NPs, rather than incorporating Ln^{3+} organic complexes into organic–inorganic hybrid hosts, as in the above examples, makes an attractive alternative for developing pure colour (*e.g.* YVO_4:Eu, $LaPO_4$:Ce and $LaPO_4$:Ce,Tb,[15] Fig. 5) and white light efficient phosphors, namely for biomedical applications. Functionalized inorganic Ln^{3+}-based NPs have been intensively investigated in the past decade, with most of the work focused on surface modification (readers interested in detailed descriptions can find specific reviews in ref. 13–15). Generally, the surface of the nanocrystals is covered by hydrophobic capping ligands (such as oleic acid, OA), which are not suitable for many biomedical and biological applications.[18] Moreover, the quantum yield values of the NPs experience a significant reduction relative to those of the corresponding bulk materials (*e.g.* 0.20 for YVO_4:Eu[15] and 0.003 for $NaYF_4$:Er,Yb[19] NPs, instead of 0.70–0.90 and 0.03 for the respective bulks). This reduction is ascribed to surface quenching effects (*e.g.* OH groups and/or solvent molecules in close proximity to the Ln^{3+} ions).[19] Therefore, surface modification of ligand-grafted inorganic Ln^{3+}-based NPs is crucial to improve their luminescence quantum yield, dispersibility and stability in aqueous solvent, and biocompatibility.[13–15,18]

Pure blue, green and red emission colours were broadly reported in the last few years also using ligand-decorated upconversion (UC) nanocrystals. UC nanocrystals are luminescent nanomaterials that convert NIR excitation into visible emission (two low energy photons are "added up" to give one high energy photon).[20] Outlined examples comprehend the blue and green emission colours of the $NaYF_4$:Yb,Er,Gd and $NaYF_4$:Yb,Tm,Gd NPs, capped with OA[20] and the reddish emission colour of the $NaYF_4$:Yb,Er NPs functionalised with diphosphonic acid, respectively.[18] Another stimulating report is the white light emission formed by the overlap of blue (450 and 475 nm, Tm^{3+}), green (545 nm, Ho^{3+}) and red (650 and 695 nm, Tm^{3+}, Ho^{3+}) UC radiations of OA-grafted $NaYF_4$:Yb, Ho, Tm nanorods. The observed UC light can be fine-tuned in a wide range of pump power densities.[21]

For applications in flat-panel displays, data storage, lighting, integrated optics, telecommunications, biolabelling and fluorescent imaging, organic-decorated Ln^{3+}-doped inorganic NPs need to be assembled in transparent composite monoliths or thin films based on polymers[14,22] or organic–inorganic hybrid structures, such as siloxane-derived hosts,[20,23–26] and sequential deposition of inorganic and organic species onto a silicon wafer.[27] In this latter example, a prototypical two-dimensional (2D) rewritable optical storage medium (with potential high-density recording capacity) has been successfully constructed by the assembly of $NaYF_4$:Yb,Er UC NPs and diarylethene (as the photochromic organic modulator). Readout wavelengths are extended to the NIR region (due to the unique excitation property of the NPs) where neither the open-ring nor the closed-ring isomers of the diarylethene show any observable absorbance, circumventing, therefore, the problem of destructive readout.[27] Another intriguing recent example showed that rationally size-tuned $NaYF_4$:Yb,Er,Gd NPs can be embedded into poly(dimethylsiloxane) monoliths in order to make volumetric three-dimensional (3D) displays, emitting in the blue-green spectral regions, presenting unique interface applications for 3D image visualization.[20]

Hybrids for lighting

Solid-state lighting is a fast growing and emerging technology whose efficiency of electricity-to-white light conversion is significantly higher than that of traditional lighting sources (approaching 50% within the next several years), besides bringing up a host of wide-spread new applications, such as, for instance, the off-grid lighting of scores of villages in developing countries, potentially providing a significant, most needed contribution for the reduction of the world's overall energy consumption.[28,29]

Commercially produced solid-state white light sources are furnished by long UV/blue GaN-based light-emitting diodes (LEDs), capped by appropriate phosphor layers (*e.g.* a yellow emitter, or a combination of a yellow/green phosphor plus a red one). Part of the blue light leaks through the phosphor layers and some is absorbed and reemitted as yellow, green and red light. The colour combination gives a warm-white light, pleasing to the human eye, displaying competitive values of luminous efficacy, colour rendering index (CRI) and correlated colour temperature (CCT), as compared to the typical values of traditional incandescent and fluorescent lighting technologies.[29] Ce^{3+} and Eu^{2+} (through the parity-allowed $5d$–$4f$ transitions) are the only lanthanide ions, which so far has proven to satisfy the solid-state lighting requirements of small Stokes energy loss, strong absorption, and short ($<10^{-6}$ s) excited state lifetimes, so as to avoid saturation under high-power density (>200 W cm^{-2}) blue LEDs excitation. Moreover, the few chemically stable and non-toxic Ce^{3+}- and Eu^{2+}-doped hosts available so far for solid-state lighting

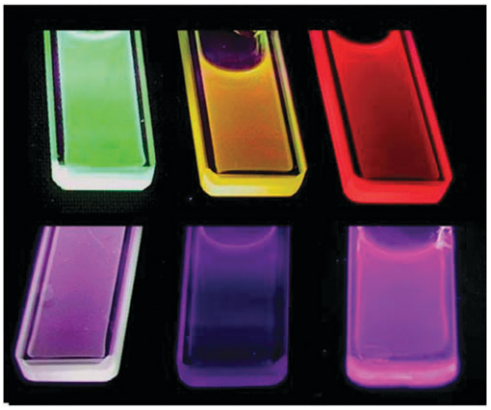

Fig. 5 Primary colors emitted by YVO_4:Eu (red), $LaPO_4$:Ce 0.7·H_2O (blue-violet), and $LaPO_4$:Ce,Tb 0.7·H_2O (green) aqueous colloids under UV excitation. (Reproduced with permission from ref. 15, copyright 2008 Elsevier.)

present some important disadvantages, such as expensive large scale synthesis, low moisture stability, thermal instability at present operating temperatures of the devices, colour deficiency in the blue-green and red spectral regions, which limits the luminous efficacy, as well as the broadband red emissions. Consequently, there have been intense efforts in the past decade with a view to developing new phosphors (both organic and inorganic), fulfilling the solid-state lighting requirements.

Organic–inorganic hybrid phosphors could be an attractive alternative to pure inorganic solids for solid-state lighting as they synergistically combine the physical properties and the functionalities of their inorganic and organic components.[30,31] From the point of view of materials science, the main challenge in solid-state lighting is the development of novel phosphors that collect the blue light from long UV/blue LEDs and efficiently convert it into the other colours needed for white light emission. The phosphors should, therefore, display the following requests:

- Ability to be synthesised and recycled in easy large scale processes;
- High brightness (luminance values >100–150 cd·m^{-2}, the typical value of the laptop screens);
- Emission quantum yield values larger than 0.50 to reduce the emitters concentration ($\sim$0.1–3.0% by weight), while retaining the integrity (transparency, mechanical and thermal stability) of the hybrid host after doping;
- Blue, yellow-green, green and red emission colours with high CRI and controlled CCT, purity and hue;
- Photostability under UV irradiation.

The development of these new phosphors for long UV-to-visible conversion will contribute to trimming down the use of Hg vapour plasma fluorescent lights (dropping the corresponding environmental contamination risks during disposal) and will also impact on the design of smart lighting with proper colour balance to mimic natural daylight. A major claim to be faced by the lighting industry is the production of smart light sources to synchronize the human circadian (wake-sleep) rhythm. The light sources should be able to be tuned in the circadian photo-sensitivity range (459–484 nm), simulating, therefore, the daylight (2000–20 000 K).[28,29] Luminous efficacy between 30 and 50 lum·W^{-1} (more than twice that of incandescent bulbs) and a colour rendering index over 80–90 are major targets that must be reached in the near future by these new cold light sources.

Concerning the processability of the lighting devices, the focus must be placed in large-scale thin film technology, namely in the hybrid/substrate and multi-layers adhesion, thickness values and homogeneity control, low surface roughness, and optical transparency.

Hybrid components for integrated optics and optical telecommunications

Photonics account for light emission and amplification within essentially the visible and NIR spectral regions. Applications have been triggered by the increasing request to expand the available telecommunication networks bandwidth at the lowest possible cost. In the 1990s the use of optical amplifiers, such as the Erbium Doped Fiber Amplifier (EDFA), brought a great development in the simplification of those systems by eliminating expensive and limitative optoelectronic regeneration. By far, the combination of optical fibres with EDFA is the transmission medium par excellence. However, the bandwidth demands have also been dramatically increased claiming for broadband amplifiers, such as Raman Fiber Amplifiers, which nowadays play an important role in high-speed/long-haul telecommunications.

To cope with the world's needs for both transmission loss and bandwidth, the EDFA gain window (conventional-wavelength band, C-band, 1530–1565 nm) must be extended to encompass the S (1460–1530 nm), and L (1565–1625 nm) transmission bands. NIR infrared amplification is also useful at shorter wavelengths, within the O (1260–1360 nm) and E (1360–1460 nm) transmission bands, because of a local minimum in the fibre optics attenuation.

In this context, the development of synthesis strategies to overcome the high non-radiative transition probability of organic group oscillators that strongly suppress the NIR Ln^{3+} emission is of major importance. NIR infrared spontaneous emissions arising from Er^{3+}, Nd^{3+}, Yb^{3+}, Tm^{3+}, Eu^{3+} and Sm^{3+} excited states have been observed in several organic–inorganic hybrids.[4,32] Examples of NIR optical amplification making use of Ln^{3+} ions are, however, scarce, owing to the presence of organic groups which remain in the Ln^{3+} surroundings after the mild temperature aging treatment, characteristic of the sol–gel process. Theoretical approaches to this problem suggest that a minimum distance of 20 Å should exist between Er^{3+} and emission quenchers, such as C–H or O–H oscillators, in order to decrease non-radiative decays.[33] A variety of strategies have been adopted to shield the ion excited levels to high non-radiative transition probability by OH, CH and/or NH oscillators:

- Design of low vibration energy deuterated or fluorinated host polymers;[34,35]
- Incorporation of Ln^{3+}-based inorganic NPs (essentially with Er^{3+} and Yb^{3+}) into organic–inorganic hybrid matrices.[23–26]

In particular, it was demonstrated that the performance of organically modified fluoroalkylene-bridged silsesquioxanes doped with Er^{3+}/CdSe NPs showed a significant reduction in absorptions at 1540 nm due to the diminution of uncondensed OH groups. Moreover, the presence of the CdSe NPs contribute to the decrease of the host photon energy, resulting in the increase of the Er^{3+} fluorescence intensity.[34]

NIR emission of Ln^{3+}-based organic–inorganic hybrids was addressed in detail in ref. 4 and 32. More recently, a series of new examples arose from the incorporation of Er^{3+}-based NPs (*e.g.* LaF_3:Er,Yb, $LaPO_4$:Er and $LaPO_4$:Er,Yb and core/shell $LaPO_4$:Er/$LaPO_4$) into hybrid frameworks (such as, MAPTMS-based and a silica-based resin prepared from GPTMS, diphenylsilanediol and phenyltrimethoxysilane).[23–26] However, few examples report the observation of NIR light signal amplification. The first report, at 1550 nm with pumping at 980 nm, was observed in channel waveguides with low OH content using an Er^{3+}-containing hybrid (based on a mixture of methyldiethoxysilane, colloidal silica and the Irgacure 819® photoinitiator) with a gain of 0.5 dB, over 7 mm.[36] More recent examples refer to: (1) OA-modified LaF_3:Er,Yb NPs embedded in PMMA. A maximum gain of ~6.8 dB at 1550 nm is observed in a 20 mm-long waveguide (pump power 120 mW at 976 nm). The waveguide also displays a bright UC green luminescence.[37] (2) $LaPO_4$:Er,Yb NPs embedded into MAPTMS modified zirconium *n*-propoxide. An optical signal enhancement of 2 dB·cm^{-1} at 1527 nm (using a 200 mW 980 nm pump laser) was measured in a 0.4 cm reverse-mesa waveguide.[32] (3) LaF_3:Er,Yb NPs containing MAPTMS-based organic–inorganic hybrids. Relative optical gains (pumping at 975–980 nm) of ~5 dB (at 1535 nm) and 2.3 dB (at 1550 nm) were measured in a 2.2 cm-long waveguide[24] and in a 1.3 cm-long reverse-mesa ridge waveguide (Fig. 6),[25] respectively.

Light amplification in the visible spectral region may find application in short haul telecommunication and fibre-to-the-home solutions. In this field, light propagation is ensured by plastic optical fibres (POFs), where propagation in the visible spectral region is required for safety purposes. One challenge for Ln^{3+}-based organic–inorganic hybrids is, therefore, light amplification in the visible spectral region. Herein, a potential market niche could be open for hybrids processing as long, thermal and mechanically stable fibres.

Nevertheless, the competitiveness of organic–inorganic hybrids, when compared with poly(methyl methacrylate), (PMMA), the main component of POFs, lies in:

- Similar attenuation values (<1 dB·cm^{-1});
- Ability to incorporate large amounts of Ln^{3+} ions, contributing to the photostability and enhancement of their emission features;[4]
- Easy and large refractive index tuneability;[32]
- Photosensitivity, allowing direct-writing;[32]
- The inclusion of PMMA as the organic counterpart;
- The siliceous network that is chemically compatible with traditional SiO_2 optical fibres.

The emission features in the visible spectral range of Ln^{3+}-containing organic–inorganic hybrids is a well demonstrated issue, in particular for the Eu^{3+} and Tb^{3+} ions due to their high quantum efficiencies (determined by the ratio between the radiative and nonradiative transition probabilities) that depend on the host vibrations' maximum frequency and on the energy gap between the lowest Stark level of each emitting multiplet and the highest Stark level of the manifold lying just below.[2,4] When the energy gap is small (*e.g.* 7500 cm^{-1} for Sm^{3+} and Dy^{3+}), it could be efficiently bridged by nonradiative processes involving the host lattice vibrational states, and the excited levels will present, in principle, low quantum efficiencies. In contrast, higher quantum efficiencies are usually observed for ions with large energy gaps (*e.g.* 12 000 and 15 000 cm^{-1} for Tb^{3+} and Eu^{3+}, respectively). Whilst light amplification and laser action in the visible spectral region have been demonstrated in several dye-doped organic–inorganic hybrids (see examples in ref. 32), these effects have not yet been reported using Ln^{3+} ions as the active centres.

Hybrids for solar cells

Solar cells (SCs) are an emerging area of application of Ln^{3+} ions. These attractive devices capture sunlight and convert it into electricity in a clean and sustainable way. In theory, one hour of sunlight is more than enough for a whole year of global consumption. However, at present, SC energy costs are not competitive and, in spite of their undeniable interest, SCs account for only 0.04% of the total energy production.[38] From the technological standpoint, the limited energy efficiency represents the most critical drawback of SCs. In conventional entirely inorganic SCs, the conversion efficiencies

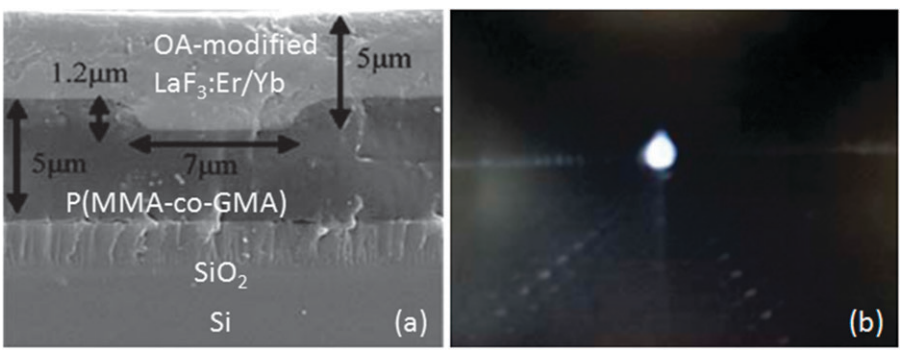

Fig. 6 (a) SEM of the reverse-mesa ridge waveguide and (b) 1550 nm signals from a 1.3 cm-long polymer waveguide. Waveguide, (P(MMA-*co*-GMA) represents (poly-methyl-methacrylate-*co*-glyciclyl-methacrylate)). (Adapted with permission from ref. 25, copyright 2008 Springer.)

have reached only 24%, the high purity materials employed are too expensive and the processing techniques are excessively energy consuming.

In recent years, organic/inorganic nanostructured hybrid SCs, combining the properties of inorganic semiconductor NPs and the properties of organic/polymer materials, have been developed as viable alternatives to SCs, based on bulk materials, such as Si.[39] The most interesting features of such SCs are not only the cheap synthesis, the easy processability and the versatile manufacturing of the thin film devices, but also the high absorption coefficients exhibited by inorganic semiconductor NPs and the fact that their optical band-gap may be easily tuned through particle size control. Among the most widely known hybrid SCs are the dye-sensitized solar cells (DSSCs)—mainly the Grätzel type ones—with solar power conversion efficiencies of 7–10% under full sun conditions. In hybrid nanomaterial-based SCs, the metal oxide (typically TiO_2) acts as the primary semiconductor and the secondary components (*e.g.*, dyes or polymers) play the role of sensitizers. In nanocrystalline SCs, organic conjugated polymers act both as transporters and sensitizers. Despite the potential advantages of nanomaterials, to date, these hybrid SCs usually display lower efficiencies than the conventional Si-based SCs. It is expected that the application of semiconductor one-dimentional (1D) nanostructures, such as nanowires, nanotubes and nanorods, to DSSCs will boost performance as a result of a smart compromise between electronic conductivity (a direct pathway for photoexcited electrons to reach the conducting substrate is provided) and specific surface area available for dye adsorption (surface area is constrained). Exciting results involving the use of TiO_2 nanotube arrays prepared by electrochemical anodization of Ti foils in DSSCs were reported recently by Kuang *et al.*[40]

Luminescent solar concentrators (LSCs) are extremely promising candidates for the production of cheaper solar electricity.[41] In a LSC a transparent flat plate doped with fluorescent organic dyes (non-toxic and inexpensive) absorbs most of the solar spectrum and the resulting high yield luminescence is emitted in the longer wavelength range of the spectrum. Repeated internal reflection of the fluorescent light in the transparent plate takes the radiation to the edges where the light concentrates and is received by SCs applied on the panel's sides.

This sort of simple but revolutionary design substantially reduces the number of SCs needed to produce a certain amount of electricity. Unlike conventional solar panels, this new generation uses diffused light instead of direct sunlight, eliminating the need for a tracking system, making easier solar integration into building. A further advantage of this technology is the good heat dissipation from the area of the collector plate, avoiding the need for cooling mechanisms. This pioneering approach, which significantly increases the efficiency and effectiveness of the light-capturing solar panels, makes solar energy economically sustainable and competitive with fossil fuels for the first time. Ideally, the collecting efficiency (*i.e.*, the amount of energy reaching the SC per energy falling on the plate) may be as high as 20%. In practice, the highest efficiency of LSCs reported so far is 7%.

At present, about 95% of the commercially available SCs are single-junction crystalline and polycrystalline Si (c-Si) systems. These devices have practical efficiencies of ~15%, although the theoretical maximum efficiency (the so-called *Schockley-Queisser limit*) of c-Si SCs with E_g = 1.1 eV is ~30%.[42] Considering the standard solar spectrum with an air mass coefficient AM1.5G (where AM is the ratio of the solar radiation path length l to the atmosphere thickness l_0, for solar radiation incident at an angle θ relative to the normal of the earth's surface, $l/l_0 = 1/\cos\theta$) and 1000 W m^{-2}, the maximum fraction of terrestrial sunlight that is effectively absorbed and employed by a thick c-Si device is 468 W m^{-2}.[42] Efficiency loss processes in single junction SCs are due to the following processes:[42] (1) lattice thermalisation; (2) transmission; (3) recombination; (4) junction; (5) contact voltage. Processes (1) and (2), usually termed *spectral mismatch* losses, account for approximately 70% of the total energy losses.

Two strategies have been proposed to reduce spectral mismatch: matching the SC to the solar spectrum (such as the method used in the so-called *tandem SCs*)[42] or matching the solar spectrum to the SC. The latter strategy may be achieved by means of UC and down-conversion (DC) mechanisms. Whereas in UC two IR photons result in one green photon (as mentioned above), in DC (or *quantum cutting*) one high energy photon is "split" into two low energy photons (one UV photon gives rise to two IR photons). If the fraction of terrestrial sunlight that is effectively absorbed and employed by a classical c-Si device is excluded, the maximum fraction of the solar radiation available for UC is 35% (164 W·m^{-2}), whereas the maximum fraction accessible for DC is 32% (149 W·m^{-2}). As the increase in the air mass coefficient of solar radiation results in a shift from the UV to the IR, DC is advantageous for solar radiation of smaller air mass coefficients (*e.g.*, extraterrestrial radiation AM0) and for diffuse terrestrial solar radiation, whereas UC is of interest for solar radiation with higher mass coefficients and for direct solar radiation.[42]

Ln^{3+}-based phosphors have been proposed as adequate up-converters and down-converters for the enhancement of the conversion efficiency of SCs. Examples of hybrid SCs including Ln^{3+}-based up-converters and down-converters are, however, scarce in the literature. Jin *et al.*[43] reported a significant enhancement of the conversion efficiency of Si-based SCs by surface coating with organically modified silicate (ormosil) phosphor films incorporating Eu^{3+}/phen and Tb^{3+}/bpy complexes. Relative maximal outputs (*i.e.*, relative light-to-electricity conversion efficiencies) of the coated single-crystal (sc-Si) and a-Si SCs, compared with those of the bare ones (defined as 100%) were increased to ~118 and ~108%, respectively, at standard conditions of the solar spectrum, owing to the effective optical conversion from the UV fraction of sunlight into visible light by the Ln^{3+}-based complexes. Machida *et al.*[44] fabricated LSC panels by coating onto uniform and transparent quartz plates 0.4 μm think $[Eu(phen)_2]Cl_3$-doped ormosils derived from TEOS and diethoxydiphenylsilane (DEDPS), displaying strong red emission and a refraction index of about 1.40. The coated phosphor successfully converted the UV component of sunlight into visible light. Connection of the coated LSC panels to c-Si SCs resulted in photovoltaic outputs 10–15% higher than those observed in systems using the bare LSC plates.

It is absolutely clear for the entire scientific community of solar energy that the embedding of Ln^{3+}-based complexes within organic–inorganic hybrid matrices will play a major key role in future LSCs. Despite the intense efforts devoted in the last few years to the development of LSCs, the systems that have been proposed so far do not entirely fulfil the requirements of photostability and efficiency.[41] One of the solutions that are envisaged to overcome these drawbacks is the use of a combination of various stable dyes, efficient quantum dots and lanthanide complexes in order to ensure that the entire solar spectrum is covered. To avoid losses due to reabsorption of the emitted light and luminescent quenching, the incorporation of the dyes/lanthanide complexes into a thin layer of a hybrid matrix in optical contact with a transparent glass plate is suggested.

Hybrids for biomedical applications

Ln^{3+}-doped organic–inorganic hybrid materials have been investigated as optical biosensors in the areas of life science, biotechnology and clinical diagnostics.[45] The interest of these functional materials relies on the combination of the solid-state properties of inorganic materials and the chemical or biofunctional behaviour of the organic moieties. Up to now, the hybrid materials investigated have involved essentially ligand-decorated Ln^{3+}-based inorganic NPs and lanthanide chelates embedded within inorganic matrices (*e.g.* silica-, gold- or silver-based NPs). Core–shell or core–corona architectures combining diverse functionalities and surface modifications into a single hybrid material have been designed as biosensing platforms for *in vivo* imaging, diagnostics, targeting and therapy.[2]

Time-resolved capability of Ln^{3+} luminescent bioprobes and the availability of adequate bioconjugation protocols allow the development of highly sensitive immunoassays. Time-resolved microscopy has also benefited from the intrinsic advantages of Ln^{3+} bioprobes and cell-penetrating optical probes, allowing not only the visualisation of live cells, but also carrying out targeted analyses of key biochemical metabolites. Extension to immunocytochemical analyses and immunohistochemical detection and therapy of cancerous tissues are now in hand.

Besides their optical characteristics, Ln^{3+} complexes also possess very specific features, such as paramagnetic properties and the ability to accumulate in cancer cells. These characteristics make them useful as a paramagnetic contrast in Magnetic Resonance Imaging (MRI) spectroscopy, in photodynamic therapy and in photodynamic cancer diagnosis.

The temperature dependence of the Ln^{3+} luminescence properties can also be used in optical sensors for temperature measurements. Among the many methods for determining temperature, luminescence-based measurements have attracted much attention as they can be non-invasive, accurate, and able to function even in strong electromagnetic fields. The advantage of optical sensors is that they are useful for thermal mapping (surface temperature distribution).

As it was stated by Soini and Hemmilä long ago,[46] the suitability of Ln^{3+} ions as biomarkers relies on their unique luminescence properties: (1) High photostability; (2) long decay rates (10^{-6}–10^{-3} s) which allow time-gate detection; (3) small Stokes shifts for the intra-4*f* transitions (<100 cm^{-1}); (4) narrow emission bands (full-width-at-half-maximum <4 nm), that make these ions very well suited for the elaboration of highly luminescent and photostable probes; and (5) easy complexation with organic ligands that allows an enhanced quantum yield *via* protection from vibrational quenching and increasing light absorption cross section by the well-known "antenna effect". These characteristics make them particularly valuable in sensors and displays, and also for fluoroimmunoassay and fluorescence microscopy. There has been growing interest also in the use of NIR light, this being one of the best strategies for acquiring high-resolution pictures of deep tissues, as NIR light diffracts much less than visible light.[47]

A promising idea investigated by Masne-de-Chermont *et al.*[48] is the use of long-lasting luminescent NPs for *in vivo* imaging. The phosphors are based on poly(ethylene glycol)-decorated $MgSiO_3$:Eu,Dy,Mn NPs (divalent europium and manganese ions), in order to ensure biocompatibility and targeting action (lung, liver or blood circulation). Moreover, as the long-lasting nanoprobes can be excited before *in vivo* injection, overcoming, therefore, the difficulties in signal analysis linked to external illumination, this breakthrough opens a whole area in bioprobes *in vivo* imaging.

The challenges concerning the use of luminescent organic–inorganic hybrid materials as biosensors are to find supporting platforms for the following properties:

- Water solubility;
- Large thermodynamic stability;
- Kinetic inertness;
- Intense absorption above 330 nm;
- Efficient energy transfer onto the Ln^{3+} ion;
- Coordination cavity minimizing non-radiative deactivations;
- Long excited-state lifetime;
- Whenever relevant, ability to conjugate with bioactive molecules while retaining its photophysical properties and not altering the bioaffinity of the host.[49]

The use of Ln^{3+} ions in biological areas has arisen as an alternative to overcome some of the limitations of traditional fluorescent biolabels, such as organic dyes, or more recently, quantum dots. The main problems that organic dyes give rise to are the broad spectral features, short lifetime, photobleaching and potential toxicity to cells.[2] Numerous studies have been devoted to solving these problems by designing versatile architectures combining diverse functionalities and surface modifications into a single hybrid nanocomposite, as biosensing platforms for *in vivo* imaging, diagnostics, targeting, therapy, nanothermometers, *etc.*

The biological chemistry of Ln^{3+} has roots in the 19th century when cerium oxalate was widely prescribed as an antiemetic drug for pregnancy sickness. Moreover, the *in vitro* antimicrobial properties of several lanthanide complexes stimulated clinical trials in the treatment of tuberculosis and leprosy, although their impact was minimal. Ln^{3+} ions also have anticoagulant properties, but their main therapeutic applications lie presently in the radioactive treatment of cancers. Gadolinium chelates are ubiquitous contrast agents for MRI and—despite some recently

reported problems with one class of compounds—they are well tolerated and considered to be harmless.

The development of Yb^{3+} luminescence for various analytical and chemosensor applications is quite promising since the typical emission of this ion occurs in the NIR region ($\sim$1000 nm) where the biological tissues and blood are relatively transparent, a crucial requirement for *in vivo* imaging.[47] Feng *et al.*[50] reported the synthesis of Fe_3O_4-based magnetic mesoporous silica (MMS) nanospheres to which the $Yb(dbm)_3$phen-MMS complex (where dbm^- stands for dibenzoylmethanide) is covalently bonded. This bimodal Yb^{3+}-based silica nanocomposite is a potential material for applications in drug delivery or optical imaging, with the following advantages:

- Mesoporous silica with a nontoxic and biocompatible nature, a large surface area, a large pore volume, and a tuneable pore diameter with abundant Si–OH bonds on the pore surface;
- NIR emission at 980 nm from $Yb(dbm)_3$phen-MMS is critical for *in vivo* optical imaging, minimizing complications resulting from intrinsic background interference;
- Yb^{3+} ions emit relatively intense NIR luminescence compared to other lanthanide ions.
- It can be guided to target sites by means of an external magnetic field.

An important aspect of the use of bioprobes for bioimaging is the ability to target them on specific organelles or receptors. A variety of receptors have been identified as markers for carcinomas. Folate receptors (FR) are important types of receptors, expressed in many of human cancerous cells (they are only minimally distributed in normal tissues), including malignancies of the ovaries, mammary glands, lungs, kidneys, brain, colon, prostate, nose, and throat. For this purpose, Hu *et al.*[51] have prepared nanocomposites of silica-coated $NaYF_4$:Yb,Er NPs containing an organic dye incorporated into the silica shell and folic acid (FA) conjugated on its surface. This material exhibits good water dispersibility, buffer stability, photostability and biocompatibility.

Another important aspect of *in vivo* imaging and biolabels has to do with the fact that biological tissues are rather transparent in the NIR spectral range and suffer less damage under excitation in such range. Therefore, materials characterized with both excitation and emission bands in the NIR region are attractive.[52] A recent example illustrating this refers to water-soluble BaFCl:Nd NPs with the surface functionalized by a layer of PAA. Under NIR excitation, these NPs display the three typical NIR intra-4*f* transitions,[3] with the most intense emission peak centred at 1055 nm. The $^4F_{3/2}$ emission decay curve is well modelled by a triple exponential curve with fitted lifetimes values of 0.58, 0.24 and 0.07 ms. Because both the excitation and major emission peaks of Nd^{3+} are present within the "optical window" of cells and tissues (spectral range of 650–1300 nm) and its $^4F_{3/2}$ lifetime value is much longer than that of cellular autofluorescence and of scattered light, BaFCl:Nd NPs might be very promising candidates as NIR fluorescent

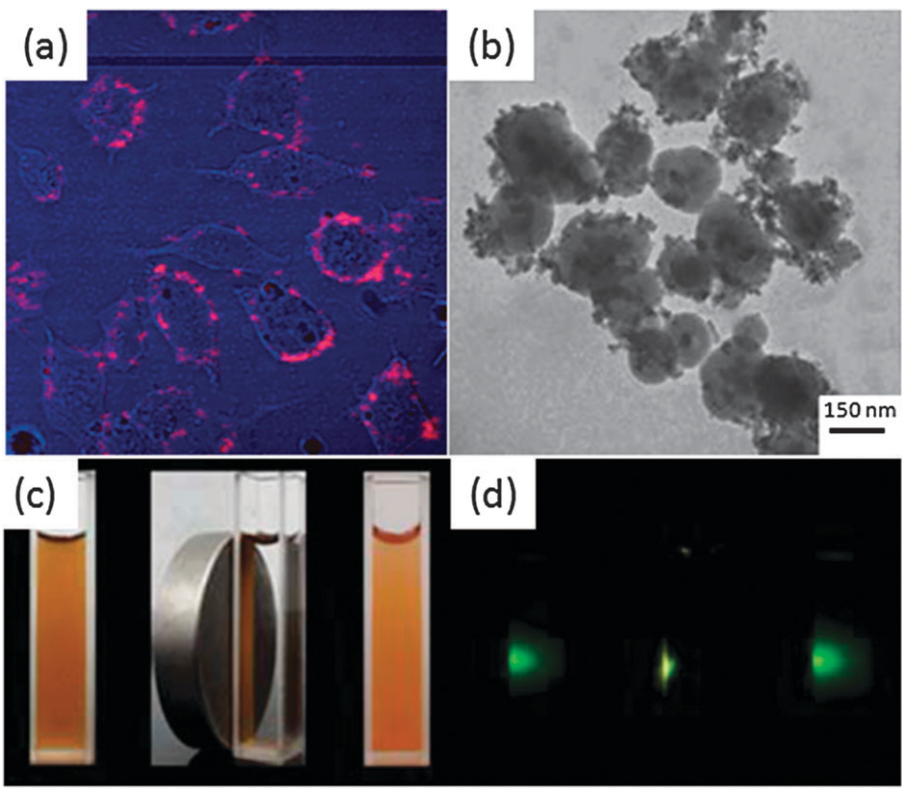

Fig. 7 (a) Confocal image of pancreatic cancer cells treated with $NaYF_4$:Er,Yb,Gd UC NPs conjugated with anti-claudin-4. (Reproduced with permission from ref. 57, copyright 2009 Wiley InterScience.) (b) TEM images of $Fe_3O_4/NaYF_4$:Yb,Er nanocomposites. (c) Bright field and (d) dark field under 980 nm excitation photographs of aqueous solution of the nanocomposites before applying a magnetic field (left), in the presence of a magnet (middle) and redispersed after removing the magnet (right). (Adapted with permission from ref. 58, copyright 2010 RSC.)

labelling agents for ultra-sensitive bioassays and bioimaging. Recent progress in the development of Ln^{3+}-based hybrid UC NPs for confocal and multiphoton microscopy have been thoroughly review by Prasad *et al.*[53] Fig. 7a illustrates a confocal image of pancreatic cancer cells targeted with anti-claudin-4-conjugated $NaYF_4$:Er,Yb,Gd UC NPs.[53]

The use of multi-functional (*e.g.* superparamagnetism, MRI, and photoluminescence) NPs introduces an innovative concept towards the simultaneous biolabelling, fluorescent imaging and MRI.[54,55] As mentioned above, NIR light avoids autofluorescence from biological media and—owing to the low absorption of NIR photons in such media—it can penetrate deep into biological tissues without causing damage and without significant loss of intensity. In carboxyl-functionalized superparamagnetic Fe_3O_4 NPs covalently linked to amino-functionalized silica-coated UC fluorescent $NaYF_4$:Yb,Er NPs the presence of both NIR-responsive and superparamagnetism enable practical applications in magnetic separation and bioimaging of HeLa cells (Fig. 7b–d).[54] On the other hand, by embedding sensitized lanthanide complexes into porous silica coated on UC $NaYF_4$ nanocrystals, three-in-one multi-functional NPs displaying DC and UC fluorescence and magnetic resonance relaxivity were obtained.[55] These $NaYF_4$:Yb,Er@Si-DTPA-4-AS-Tb,Gd multi-functional NPs (where DTPA—diethylenetriaminepenta-acetic acid—was coupled to APTS to form the Si-DTPA-4-AS silanized complex) exhibit DC and UC luminescence, longitudinal R_1 and transverse R_2 magnetic relaxivities and an interesting fluorescence resonance energy transfer mechanism from the UC nanocrystals to the DTPA-4-AS sensitizer.[55]

Two years ago Chatteriee *et al.*[56] used UC fluorophores with excitation in the NIR region for *in vitro* imaging of human cells and, for the first time, for *in vivo* imaging in tissues of small mammals. The fluorophores proposed were $NaYF_4$ NPs coated with high molecular weight poly(ethyleneimine) (PEI). The presence of the polymer amine groups render the NPs water soluble and enable their covalent bonding to biomolecules. The PEI-coated NPs are stable in physiological phosphate-buffered saline, non-toxic to bone marrow stem cells, and resistant to photo-bleaching. When exposed to a 980 nm NIR laser, FA-coated PEI/$NaYF_4$ NPs delivered to human HT29 adenocarcinomacells and human OVCAR3 ovarian carcinoma cells showed visible fluorescence. PEI-coated NPs, injected intradermally and intramuscularly into some tissues of rats, either near the body surface or deep into the body, exhibited visible fluorescence from a depth of up to 10 mm, when excited at 980 nm (Fig. 8).[56]

Molecular thermometers

Temperature is the most frequently measured physical property in both science and industry. Most optical methods for measuring temperature can be grouped into two categories.[51,57,58] The first type of measurements are based on the temperature dependence of the absorption (or the reflection) of certain materials. Examples of this method include thermochromic materials, gas band edge absorptions that shift with temperature, Fabry-Perot interferometers, and changes in refractive indexes. The second category of measurements is based on luminescence temperature dependence, such as changes in energy, intensity, or decay lifetime.

The production of biological temperature sensors must take into account that the temperature of a living cell is changeable during every cellular event, such as cell division, gene expression, enzyme reaction, and metabolism. From a clinical viewpoint, pathological cells are warmer than normal cells due to their enhanced metabolic activity. Thus, measuring cellular temperature, may contribute to the explanation of intricate biological processes and the development of novel diagnoses.[59]

Sensors are also needed, for example, in hyperthermal tumour treatment and in photodynamic cancer therapy, because knowing the temperature of the targeted tissue is of the greatest importance in order to achieve optimal therapeutic results. Although well known and commercially available, fibre-optic luminescence-based temperature sensors are not suitable for contactless intracellular measurements and temperature imaging. Cellular temperature determination has been seldom reported so far, most likely because of the scarcity of biocompatible and small-sized sensors.[59]

Changes in temperature induce changes in luminescence intensity and lifetime. Intensity-based methods must use the ratio between the intensity of two transitions of the same phosphor, instead of only one transition. The main advantage of this technique, known as fluorescence intensity ratio (FIR), is the fact that a single emission spectrum contains all the information needed to compute the absolute temperature. The FIR ratio employs a Boltzmann distribution of electrons between adjacent emitting energy levels that is a function of temperature and is manifested as a temperature-dependent intensity ratio between emissions from two distinct lines in the spectrum. The FIR algorithm makes the temperature sensing independent of the probe concentration and of the drifts of the optoelectronic system (lamp and detectors), overcoming, then, the main drawbacks of the intensity-based measurements of only one transition. Generally, FIR is preferable in temperature sensor applications over lifetime measurements. Although such measurements are also neither affected by the intensity of the excitation source nor by the probe concentration, they are time-consuming requiring sophisticated setups and post-processing computational treatment.

G. E. Khalil *et al.*[57] have given a detailed description of the use of Eu^{3+}-diketonate complexes as temperature sensors since Eu^{3+}-based chelates display a highly temperature-dependent emission, large Stokes' shifts, and long lifetimes. Among the various known probes, Eu^{3+}-based chelates, exhibiting sensitized luminescence which can be excited with visible light, are advantageous over UV-excitable probes for the following reasons, among others:

- Long-wave excitation strongly reduces the background fluorescence of biomatter;
- Visible excitation is less prone to interferences by inner filter effects due to absorption of light;
- Long-wave UV and visible excitation has become possible, in recent years, due to the availability of inexpensive and portable LEDs and diode-laser light sources.

However, such sensors have limitations when measuring temperature in the physiological range (25–45 °C) or inside cells due to limited spatial resolution, inadequate temperature

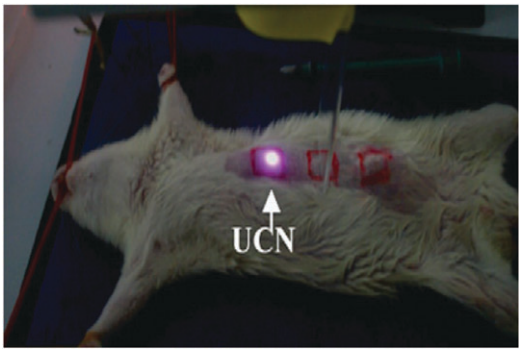

Fig. 8 Fluorescence imaging of deep tissues in a small rat using PEI/$NaYF_4$:Yb,Er NPs injected subcutaneously below abdominal skin (Adapted with permission from ref. 59, copyright 2008 Elsevier.)

resolution, and slow response (due to their large size). Recent advances in nano and biotechnology enable the miniaturization of luminescent thermometers down to the micro and nanoscale regimes, with high spatial resolution using Ln^{3+}-based organic–inorganic hybrids.[60,61]

Peng *et al*. reported siloxane hybrid NPs (size ranging from 20 to 30 nm) incorporating an Eu^{3+} tris(β-diketonate) complex displaying strong temperature dependence in both luminescence intensity and $^5D_0$ lifetime over the physiological range (25–45 °C), illustrating, therefore, the ability for sensing and imaging physiological temperatures.[60] Another recent example of luminescent molecular thermometers was reported by Brites *et al*.[61] They have prepared organic–inorganic hybrids co-doped with [Eu(btfa)$_3$(MeOH)(bpeta)] and [Tb(btfa)$_3$(MeOH)(bpeta)] β-diketonate chelates (where btfa$^-$, bpeta and MeOH represent, respectively, 4,4,4-trifluoro-1-phenyl-1,3-butanedionate), 1,2–bis-(4–pyridyl)ethane and methanol) combining:

- Self-referencing allowing absolute measurements;
- 4.9%·K^{-1} maximum temperature sensitivity (better than 0.5%·K^{-1} in the physiological temperature range);
- High photostability for long-term use;
- Ability to fine-tune emission colour as a function of temperature, Eu^{3+}/Tb^{3+} proportion and hybrid host;
- Flexibility to be processed as thin films for sensing/mapping large areas with a spatial resolution limited by the size of the optical detectors (~1–10 μm for commercial optical fibres and CCD cameras);
- A temperature uncertainty of 0.5 degrees;
- Multifunctionality, as it can be hosted in silica-coated magnetic NPs.

When comparing this thermometer (Fig. 9) with the Ln^{3+}-based ones proposed so far, it is clear that it represents a step forward in thermometry at the nanoscale. The synergy resulting from combining temperature sensing/mapping and superparamagnetism opens the way for new exciting applications, especially in the biomedical field. In particular, such association will provide a unique instrument to map, in a non-invasive way, temperature distributions in biological tissues (*e.g.*, in tumours) during heat release, due to the application of an ac field to magnetic NPs (magnetic hyperthermia), this being, undoubtedly, a powerful tool for the study of biochemical micro-processes occurring within a cell.

Conclusions

The examples of applications of Ln^{3+}-based organic–inorganic hybrids described in this tutorial review emphasise the emergent impact of these multifunctional advanced materials in countless aspects of phosphor technology, lighting, integrated optics, optical telecommunications, solar cells, and biosciences.

Whereas in phosphor technology we highlight the development of (1) efficient blue emitters and (2) hybrid materials that collect the light from long UV/blue LEDs and convert it into other colours needed for white light emission, in integrated optics and optical telecommunications, we accentuate the processing of Ln^{3+}-based hybrids as long, thermally and mechanically stable fibres for short haul telecommunication and fibre-to-the-home solutions. In solar cells, once the technology of LSCs is developed to produce electricity from solar energy at the same cost as from fossil fuels, the industry will undoubtedly experience a revolution with unforeseen implications in peoples' quality of life. Finally, in life sciences,

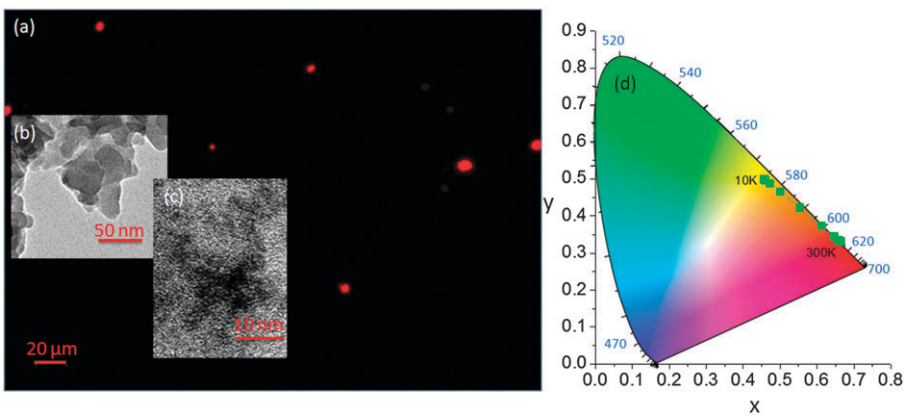

Fig. 9 Optical microscope image (UV excitation at 365 nm) of multifunctional hybrid NPs formed by a supermagnetic core coated with a TEOS/APTES organosilica shell embedding a luminescent molecular thermometer. The red colour corresponds to the real colour. (b) TEM image with a general view of the NPs showing aggregation occurred probably during the evaporation of the dispersion on the grid. (c) Amplification TEM image of the iron oxide core. (d) CIE chromaticity diagram showing the temperature dependence of the (x,y) color coordinates of the molecular thermometer.

the development of multifunctional materials simultaneously exhibiting different properties introduces an innovative concept towards dual biolabelling and fluorescent imaging. For *in vivo* imaging, the research is mainly focused on the study of multifunctional UC materials, which are excited in the NIR spectral range, where biological tissues are rather transparent. The most highlighted investigations are nowadays addressed towards the internalization of UC phosphors and the surface functionalization with biomolecules acting as receptors to target specific organs. Furthermore, new synthetic methodologies that increase efficiency of UC mechanisms should focus on the chemical/thermal stability of the NPs under high-power NIR excitation, where unwanted laser ablation of NPs occurs. The hybrid host may play a crucial role for the NPs stabilization acting as a thermal dissipator (*e.g.* hybrid aerogels prepared under supercritical drying conditions).

Similarly, new luminescent molecular thermometers based on Ln^{3+}-doped organic–inorganic hybrids able to associate different properties (temperature sensing/mapping and superparamagnetism) in a unique material, represent an exceptional instrument to map, in a non-invasive way, temperature distributions in biological tissues.

The integration and complementarity of different active and passive hybrid components—partially or totally assembled into more complex architectures—for sensing purposes (*e.g.* temperature, humidity, RF-signals) is clearly one of the next evolutionary steps in this research area with dramatic impact on information and communication technologies, global health and biomedicine, structural engineering and environment monitoring systems. This sort of "lab-on-a-chip technology", which is expected to soon become an important part of mankind's daily life, faces many challenges, such as speed, sensitivity, specificity, ease of use, shelf life, cost, scalability and recyclability. Organic–inorganic hybrid materials (in particular, embedding lanthanide ions) will become increasingly sophisticated, miniaturized, eco-friendly, energetically efficient, reliable, and inexpensive and will undoubtedly play a key role in this cutting-edge technological endeavour.

Acknowledgements

We acknowledge Fundação para a Ciência e a Tecnologia (FCT, Portugal), FEDER and COMPETE programs (PTDC/CTM/72093/06, PTDC/CTM/101324/08). The work at Universitat Jaume I (Castellón) has been supported by the Spanish Government (MAT 2008-03479) and Bancaixa Foundation-Universitat Jaume I (P1 1B2007-47) projects. L.D.C. wishes to express sincere gratitude to A.L.L. Videira for his invaluable assistance, deep interest in and support of the author career, and, mostly, for the privilege of his friendship. B.J.-L. is especially thankful to Ministerio de Ciencia e Innovación for her "Ramón y Cajal" contract.

Notes and references

1 C. Sanchez, B. Julian, P. Belleville and M. Popall, *J. Mater. Chem.*, 2005, **15**, 3559–3592.
2 P. Escribano, B. Julian-Lopez, J. Planelles-Arago, E. Cordoncillo, B. Viana and C. Sanchez, *J. Mater. Chem.*, 2008, **18**, 23–40.
3 K. Binnemans, *Chem. Rev.*, 2009, **109**, 4283–4374.
4 L. D. Carlos, R. A. S. Ferreira, V. de Zea Bermudez and S. J. L. Ribeiro, *Adv. Mater.*, 2009, **21**, 509–534.
5 L. D. Carlos, Y. Messaddeq, H. F. Brito, R. A. S. Ferreira, V. de Zea Bermudez and S. J. L. Ribeiro, *Adv. Mater.*, 2000, **12**, 594–598.
6 L. D. Carlos, R. A. Ferreira, J. P. Rainho and V. de Zea Bermudez, *Adv. Funct. Mater.*, 2002, **12**, 819–823.
7 L. Armelao, S. Quici, F. Barigelletti, G. Accorsi, G. Bottaro, M. Cavazzini and E. Tondello, *Coord. Chem. Rev.*, 2010, **254**, 487–505.
8 J. L. Liu, B. Yan and L. Guo, *Eur. J. Inorg. Chem.*, 2010, 2290–2296.
9 D. Zhao, S. J. Seo and B. S. Bae, *Adv. Mater.*, 2007, **19**, 3473–3479.
10 S. S. Park, B. An and C. S. Ha, *Microporous Mesoporous Mater.*, 2008, **111**, 367–378.
11 K. Lunstroot, K. Driesen, P. Nockemann, K. Van Hecke, L. Van Meervelt, C. Gorller-Walrand, K. Binnemans, S. Bellayer, L. Viau, J. Le Bideau and A. Vioux, *Dalton Trans.*, 2009, 298–306.
12 S. M. Bruno, R. A. S. Ferreira, F. A. A. Paz, L. D. Carlos, M. Pillinger, P. Ribeiro-Claro and I. S. Goncalves, *Inorg. Chem.*, 2009, **48**, 4882–4895.
13 F. Wang and X. G. Liu, *Chem. Soc. Rev.*, 2009, **38**, 976–989.
14 C. X. Li and J. Lin, *J. Mater. Chem.*, 2010, **20**, 6831–6847.
15 J. P. Boilot, T. Gacoin and S. Perruchas, *C. R. Chim.*, 2010, **13**, 186–198.
16 P. P. Lima, F. A. A. Paz, R. A. S. Ferreira, V. de Zea Bermudez and L. D. Carlos, *Chem. Mater.*, 2009, **21**, 5099–5111.
17 Y. Wang, H. R. Li, Y. Feng, H. J. Zhang, G. Calzaferri and T. Z. Ren, *Angew. Chem. Int. Edit.*, 2010, **49**, 1434–1438.
18 H. Schafer, P. Ptacek, K. Kompe and M. Haase, *Chem. Mater.*, 2007, **19**, 1396–1400.
19 J. C. Boyer and F. C. J. M. van Veggel, *Nanoscale*, 2010, **2**, 1417–1419.
20 F. Wang, Y. Han, C. S. Lim, Y. H. Lu, J. Wang, J. Xu, H. Y. Chen, C. Zhang, M. H. Hong and X. G. Liu, *Nature*, 2010, **463**, 1061–1065.
21 L. W. Yang, H. L. Han, Y. Y. Zhang and J. X. Zhong, *J. Phys. Chem. C*, 2009, **113**, 18995–18999.
22 J. C. Boyer, N. J. J. Johnson and F. C. J. M. van Veggel, *Chem. Mater.*, 2009, **21**, 2010–2012.
23 B. Y. Ahn, S. I. Seok, S. I. Hong, J. S. Oh, H. K. Jung and W. J. Chung, *Opt. Mater.*, 2006, **28**, 374–379.
24 D. Zhang, C. Chen, C. M. Chen, C. S. Ma, D. M. Zhang, S. Bo and Z. Zhen, *Appl. Phys. Lett.*, 2007, **91**, 161109.
25 S. Bo, J. Wang, H. Zhao, H. Ren, Q. Wang, G. Xu, X. Zhang, X. Liu and Z. Zhen, *Appl. Phys. B: Lasers Opt.*, 2008, **91**, 79–83.
26 M. A. Lim, S. Il Seok, W. J. Chung and S. I. Hong, *Opt. Mater.*, 2008, **31**, 201–205.
27 C. Zhang, H. P. Zhou, L. Y. Liao, W. Feng, W. Sun, Z. X. Li, C. H. Xu, C. J. Fang, L. D. Sun, Y. W. Zhang and C. H. Yan, *Adv. Mater.*, 2010, **22**, 633–637.
28 E. F. Schubert and J. K. Kim, *Science*, 2005, **308**, 1274–1278.
29 C. J. Humphreys, *MRS Bull.*, 2008, **33**, 459–470.
30 J. D. Furman, A. Y. Warner, S. J. Teat, A. A. Mikhailovsky and A. K. Cheetham, *Chem. Mater.*, 2010, **22**, 2255–2260.
31 S. S. Nobre, X. Cattoen, R. A. S. Ferreira, M. W. C. Man and L. D. Carlos, *Phys. Status Solidi RRL*, 2010, **4**, 55–57.
32 R. A. S. Ferreira, P. S. André and L. D. Carlos, *Opt. Mater.*, 2010, 1397–1409.
33 F. Quochi, R. Orru, F. Cordella, A. Mura, G. Bongiovanni, F. Artizzu, P. Deplano, M. L. Mercuri, L. Pilia and A. Serpe, *J. Appl. Phys.*, 2006, **99**, 053520.
34 K. M. Choi, *Mater. Chem. Phys.*, 2007, **103**, 176–182.
35 S. Moynihan, R. Van Deun, K. Binnemans and G. Redmond, *Opt. Mater.*, 2007, **29**, 1821–1830.
36 P. Etienne, P. Coudray, J. Porque and Y. Moreau, *Opt. Commun.*, 2000, **174**, 413–418.
37 D. Zhang, C. Chen, F. Wang and D. M. Zhang, *Appl. Phys. B: Lasers Opt.*, 2010, **98**, 791–795.
38 L. M. Gonçalves, V. de Zea Bermudez, H. A. Ribeiro and A. M. Mendes, *Energy Environ. Sci.*, 2008, **1**, 655–667.
39 S. Guenes and N. S. Sariciftci, *Inorg. Chim. Acta*, 2008, **361**, 581–588.
40 D. Kuang, J. Brillet, P. Chen, M. Takata, S. Uchida, H. Miura, K. Sumioka, S. M. Zakeeruddin and M. Gratzel, *ACS Nano*, 2008, **2**, 1113–1116.

41 R. Reisfeld, *Opt. Mater.*, 2010, **32**, 850–856.
42 B. M. van der Ende, L. Aarts and A. Meijerink, *Phys. Chem. Chem. Phys.*, 2009, **11**, 11081–11095.
43 T. Jin, S. Inoue, K. Machida and G. Adachi, *J. Electrochem. Soc.*, 1997, **144**, 4054–4058.
44 K. Machida, H. Li, D. Ueda, S. Inoue and G. Adachi, *J. Lumin.*, 2000, **87–89**, 1257–1259.
45 J. C. G. Bünzli, *Chem. Rev.*, 2010, **110**, 2729–2755.
46 E. Soini and I. Hemmila, *Clin. Chem.*, 1979, **25**, 353–361.
47 J. Zhang, P. D. Badger, S. J. Geib and S. Petoud, *Angew. Chem., Int. Ed.*, 2005, **44**, 2508–2512.
48 Q. Le Masne de Chermont, C. Chaneac, J. Seguin, F. Pelle, S. Maitrejean, J. P. Jolivet, D. Gourier, M. Bessodes and D. Scherman, *Proc. Natl. Acad. Sci. U. S. A.*, 2007, **104**, 9266–9271.
49 S. V. Eliseeva and J. C. G. Bünzli, *Chem. Soc. Rev.*, 2010, **39**, 189–227.
50 J. Feng, S. Y. Song, R. P. Deng, W. Q. Fan and H. J. Zhang, *Langmuir*, 2010, **26**, 3596–3600.
51 H. Hu, L. Q. Xiong, J. Zhou, F. Y. Li, T. Y. Cao and C. H. Huang, *Chem.–Eur. J.*, 2009, **15**, 3577–3584.
52 Q. Ju, W. Luo, Y. Liu, H. Zhu, R. Li and X. Chen, *Nanoscale*, 2010, **2**, 1208–1212.
53 T. Y. Ohulchanskyy, I. Roy, K. T. Yong, H. E. Pudavar and P. N. Prasad, *Wires Nanomed. Nanobi.*, 2010, **2**, 162–175.
54 C. Mi, J. Zhang, H. Gao, X. Wu, M. Wang, Y. Wu, Y. Di, Z. Xu, C. Mao and S. Xu, *Nanoscale*, 2010, **2**, 1141–1148.
55 Z. Li and Y. Zhang, *Nanoscale*, 2010, **2**, 1240–1243.
56 D. K. Chatteriee, A. J. Rufalhah and Y. Zhang, *Biomaterials*, 2008, **29**, 937–943.
57 G. E. Khalil, K. Lau, G. D. Phelan, B. Carlson, M. Gouterman, J. B. Callis and L. R. Dalton, *Rev. Sci. Instrum.*, 2004, **75**, 192–206.
58 J. Lee and N. A. Kotov, *Nano Today*, 2007, **2**, 48–51.
59 C. Gota, K. Okabe, T. Funatsu, Y. Harada and S. Uchiyama, *J. Am. Chem. Soc.*, 2009, **131**, 2766–2767.
60 H. S. Peng, M. I. J. Stich, J. B. Yu, L. N. Sun, L. H. Fischer and O. S. Wolfbeis, *Adv. Mater.*, 2010, **22**, 716–719.
61 C. D. S. Brites, P. P. Lima, N. J. O. Silva, A. Millán, V. S. Amaral, F. Palacio and L. D. Carlos, *Adv. Mater.*, 2010, 4499–4504.